Applied Physics Letters

Shubnikov–de Haas oscillations and Rashba splitting in Bi_2Te_3 epitaxial film

Cite as: Appl. Phys. Lett. **117**, 102108 (2020); https://doi.org/10.1063/5.0019081
Submitted: 21 June 2020 . Accepted: 28 August 2020 . Published Online: 11 September 2020

D. P. A. Holgado, K. Bolaños, S. de Castro, H. S. A. Monteiro, F. S. Pena, A. K. Okazaki, C. I. Fornari, P. H. O. Rappl, E. Abramof, D. A. W. Soares, and M. L. Peres

AIP Publishing

Applied Physics Letters ARTICLE scitation.org/journal/apl

Shubnikov–de Haas oscillations and Rashba splitting in Bi_2Te_3 epitaxial film

Cite as: Appl. Phys. Lett. **117**, 102108 (2020); doi: 10.1063/5.0019081
Submitted: 21 June 2020 · Accepted: 28 August 2020 ·
Published Online: 11 September 2020

D. P. A. Holgado,[1] K. Bolaños,[1] S. de Castro,[2] H. S. A. Monteiro,[1] F. S. Pena,[1] A. K. Okazaki,[3] C. I. Fornari,[4] P. H. O. Rappl,[3] E. Abramof,[3] D. A. W. Soares,[1] and M. L. Peres[1,a)]

AFFILIATIONS

[1]Instituto de Física e Química, Universidade Federal de Itajubá, Itajubá, MG CEP 37500-903, Brazil
[2]Universidade do Estado de Minas Gerais, Divinópolis, MG CEP 35501-170, Brazil
[3]Laboratório Associado de Sensores e Materiais, Instituto Nacional de Pesquisas Espaciais, São José dos Campos, SP CEP 12227-010, Brazil
[4]Experimentelle Physik VII, Universität Würzburg, Am Hubland, 97074 Würzburg, Germany

[a)]**Author to whom correspondence should be addressed**: marcelos@unifei.edu.br

ABSTRACT

This work presents the results of magnetotransport measurements performed on a 156 nm-thick Bi_2Te_3 epitaxial film in the temperature range of 1.9–300 K, showing Shubnikov–de Haas oscillations for temperatures below 50 K. A detailed analysis of oscillations as a function of temperature provides the main transport parameters, including the Landé g-factor and cyclotronic masses. A systematic analysis of fast Fourier transform, performed on the oscillations, indicates that the origin of the oscillation pattern is not related to the topological surface states but from the Rashba splitting of the Bi_2Te_3 Fermi surface.

Bi_2Te_3 is part of a material group classified as topological insulators (TIs) that presents natural spin-polarized currents composed of Dirac fermion particles that flow via topological surface states (TSS). Such properties make Bi_2Te_3 compounds potential candidates for application in spintronics and quantum computation, which led to an intense investigation of its optical and transport properties in the past decade.[1–4] The TSS result from the spin-momentum locking due to the strong spin–orbit coupling (SOC) intrinsic to these materials and their detection via transport measurements is mandatory for rapid implementation in integrated circuits. However, this is a complex task because of the Bi_2Te_3 strong degenerate nature, since transport via bulk and surface states is mixed due to the Fermi level resonance in the bands. This is mainly due to the unintentional doping of crystal defects (antisite or point defects).[5] Magnetotransport measurements are an important tool to investigate the existence of such states since the Shubnikov–de Haas (SdH) oscillations afford a significant role in identifying the contribution of TSS conduction. From the SdH oscillation angle dependence and the magnetic field dependence of the Landau levels (LLs), it is possible to identify the Dirac fermion presence in most topological insulators. However, in the Bi_2Te_3 case, the bulk cylindrical Fermi surface can also give rise to 2D quantum oscillations. In addition, due to the cylindrical Fermi surface, the SdH frequency follows the dependency $F \propto 1/\cos\theta$, also commonly attributed to Dirac fermions.[6] From LL analysis, the Dirac fermions are expected to exhibit a non-zero Berry phase, while normal fermions have a zero Berry phase. It has recently been shown that the Rashba splitting of the cylindrical Fermi surface could also give rise to the non-zero Berry phase[7] that, in this case, has nothing to do with TSS. Despite the intensive investigation of the electrical and optical properties carried out over the past few years, very few information regarding the experimental investigation of the Rashba effect on Bi_2Te_3 based structures is found in the literature.

In this work, we present the analysis of the magnetoresistance measurements performed in an *n*-type Bi_2Te_3 epitaxial film, which presented SdH oscillations in the temperature range of 1.9–50 K. The detailed investigation of the frequencies obtained from FFT (fast Fourier transform) revealed two main peaks, which are attributed to the Rashba effect that splits the bulk states leading to the oscillation patterns observed in the experiments. This scenario corroborates the analysis of the Fermi surface provided by the angle dependence of SdH oscillations. From FFT analysis and SdH oscillation amplitude, we obtained the cyclotronic masses, the effective Landé *g*-factor, and

the Rashba splitting Δk_R and Rashba coefficient α_R. The results show that, even though the investigated sample presented the features of transport via TSS, the complex form of the Bi_2Te_3 Fermi surface, together with the Rashba splitting, is the most likely cause of the quantum oscillations observed in the experiments. In addition, the high value of α_R, when compared to similar structures, opens the possibility of the application of a tunable Rashba effect by means of a disorder induced by exposure to environmental conditions.

Sample preparation was performed on a Riber 32P MBE system, using a Bi_2Te_3 solid source, with nominal stoichiometry. The electric contact preparation followed the van der Pauw geometry, using gold (Au) wires soldered with indium (In) contacts. Details about the MBE growth of Bi_2Te_3 epitaxial films on the BaF_2 (111) substrates are published elsewhere.[8] The magnetoresistance measurements were performed using a Physical Property Measurement System from Quantum Design composed of a He-cooled superconducting system with a magnetic field of up to 9 T and an operating temperature of 1.9 K–400 K.

Figure 1(a) shows the longitudinal electrical resistance (R_{xx}) as a function of temperature for the 156 nm-thick Bi_2Te_3 epitaxial film in the temperature range of 1.9–300 K. According to this figure, the sample exhibits a metallic behavior, which agrees with the highly degenerate Bi_2Te_3 films reported in the literature.[9] Figure 1(b) shows the carrier mobility (left axis, open circles) and concentration (right axis, open squares), where it is possible to observe that carrier concentration is nearly constant for $T < 10$ K, indicating that the Fermi level energy is also constant. In the same temperature region, it is possible to observe that carrier mobility saturates for $T < 10$ K, indicating that no additional scattering mechanism becomes effective in this temperature region. The inset in Fig. 1(b) shows the linear profile of the Hall resistance R_{xy} at 4.2 K. Such linear behavior indicates that only a single band contributes to the electrical transport.

Figure 2(a) shows R_{xx} as a function of the magnetic field applied perpendicularly to the sample surface. In this figure, small-amplitude oscillations are observed for magnetic fields above 6 T and temperatures below 50 K. Quantum oscillations can be better resolved if the second derivative, with relation to the magnetic field, is applied to R_{xx}. The curve of d^2R_{xx}/dB^2 as a function of the magnetic field is shown in the inset of Fig. 2(a) for $T = 4.2$ K, where the presence of the Shubnikov–de Haas effect is clear. In Fig. 2(b), we plot d^2R_{xx}/dB^2 as a function of the inverse of the magnetic field for different temperatures. As expected, the amplitude of the SdH oscillations decreases with increasing temperature, and for $T = 50$ K, the oscillations almost disappear. From this figure, it is possible to observe that the SdH oscillations have at least two components with different frequencies since a beating pattern is visible. The frequencies responsible for the beating pattern can be obtained by applying FFT analysis. The FFT curves are displayed in Fig. 3(a) showing the presence of two well-developed peaks with frequencies $f_1 = 59$ T and $f_2 = 75$ T close to each other. From these frequencies, we can calculate the carrier concentrations by $n_{SdH} = k_F{}^3/3\pi^2$, where k_F is the Fermi wave vector that can be calculated using $k_F = (2ef/\hbar)^{1/2}$. We obtain $n_{SdH} = 2.5 \times 10^{18}$ cm^{-3} and $n_{SdH} = 3.7 \times 10^{18}$ cm^{-3} for f_1 and f_2, respectively. The carrier concentration derived from Hall measurements was $n_{Hall} = (2.1 \pm 0.1) \times 10^{18}$ cm^{-3} close to the values obtained from the SdH frequencies.

Further analysis of the SdH oscillations allows us to extract important parameters. From the temperature dependence of the FFT amplitude, we can obtain the cyclotron masses according to the thermodynamic term of the Lifshitz–Kosevich (LK) equation,

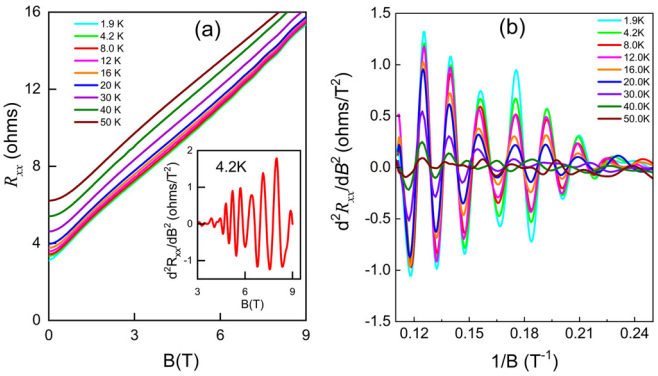

FIG. 2. (a) Longitudinal resistance R_{xx} as a function of the magnetic field applied perpendicularly to the sample surface. Small-amplitude oscillations are observed for magnetic fields above 6 T and temperatures below 30 K. Inset: d^2R_{xx}/dB^2 as a function of the magnetic field at 4.2 K where quantum oscillations are clear. (b) SdH oscillations obtained by the second derivative of R_{xx} with respect to B as a function of $1/B$.

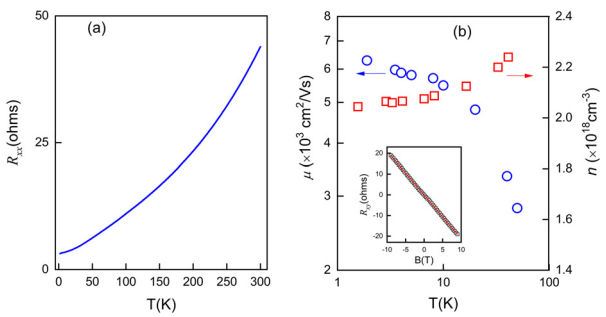

FIG. 1. (a) Temperature dependence of longitudinal resistance R_{xx} for the Bi_2Te_3 film. The profile indicates metallic behavior. (b) Carrier mobility (left axis, open circles) and concentration (right axis, open squares). The inset shows Hall resistance R_{xy} at 4.2 K as a function of B. The solid red curve is a linear fit to the data.

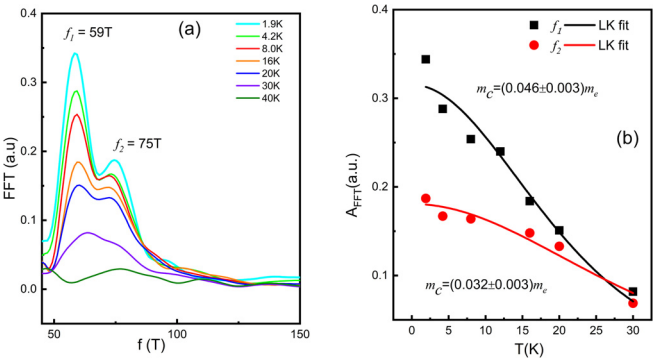

FIG. 3. (a) Fast Fourier transform (FFT) curves obtained from the SdH oscillations at different temperatures. (b) Temperature dependence of the FFT amplitude of each frequency. The solid lines are fittings using the thermodynamic term of the LK equation.

$$A_{FFT} = A_0\left(\frac{2\pi^2 k_B}{e\hbar}\frac{m_c T}{\overline{B}}\right)/\sinh\left(\frac{2\pi^2 k_B}{e\hbar}\frac{m_c T}{\overline{B}}\right), \quad (1)$$

where A_0 is a constant parameter, k_B is the Boltzmann constant, e is the elementary charge, $\hbar$ is the reduced Planck constant, T is the temperature, $\overline{B}$ is the inverse of the mean value of the $1/B$ range used in the FFT analysis, and m_c is the cyclotron effective mass. The calculations were carried out considering the interval of 0.11–0.35 T^{-1}. The obtained cyclotron masses are $m_c/m_e = 0.046 \pm 0.003$, for the peak with $f_1 = 59$ T and $m_c/m_e = 0.032 \pm 0.003$ for the peak with $f_2 = 75$ T. The fittings using Eq. (1) are shown in Fig. 3(b).

There are some explanations available in the literature concerning the two frequencies observed in Bi_2Te_3 films. The second harmonic or bulk states are possible causes. As discussed before, the two frequencies are very close to each other and the second harmonic situation is discarded. Another alternative is to consider that the surface states can contribute to transport. In this case, transport through the sample would be a composition of normal fermions, from bulk, and Dirac fermions, from surface states. A more precise procedure would be the use of the complete Lifshitz–Kosevich expression to fit the normalized oscillatory component $\Delta R_{xx}/R_0$ to obtain the Berry phase,[10]

$$\frac{\Delta R_{xx}}{R_0} = \left(\frac{\hbar\omega_c}{2E_F}\right)^{\frac{1}{2}}\frac{\chi}{\sinh(\chi)}e^{-\chi_D}\cos\left[2\pi\left(\frac{E_F}{\hbar\omega_c}+\frac{1}{2}+\beta-\delta\right)\right], \quad (2)$$

where E_F is the Fermi energy given by $E_F = \hbar^2 {k_F}^2/2m_c$, k_F is the Fermi wavevector, $\chi = 2\pi^2 k_B T/\hbar\omega_c$, and $\chi_D = 2\pi^2 k_B T_D/\hbar\omega_c$, the cyclotron frequency is given by $\omega_c = eB/m_c$ and T_D is the Dingle temperature, which provides the low-temperature collision broadening of electron states at the Fermi level giving information about crystal quality. The phase shift δ gives the dimensionality of the Fermi surface. $\delta = 0$ indicates that the Fermi surface is 2D, while $\delta = -1/8$ or $+1/8$, the Fermi surface is 3D. The phase parameter β can assume values in the range from 0 to 1. For $\beta = 0$ or $\beta = 1$, trivial fermions should be the main carriers responsible for transport. For $\beta = 1/2$, Dirac fermions should give a more effective contribution for conductivity.

From the fitting performed in our data using Eq. (2) (see Fig. S1, in the supplementary material), the obtained parameters are $\beta_1 - \delta = 0.59 \pm 0.01$ ($f_1 = 59$ T), $\beta_2 - \delta = 0.57 \pm 0.01$ ($f_2 = 75$ T), $T_{D1} = 44$ K, and $T_{D2} = 68$ K. We also extracted the values of mobility, $\mu_1 = (1056 \pm 71)$ cm^2 V^{-1} s^{-1} and $\mu_2 = (981 \pm 92)$ cm^2 V^{-1} s^{-1}, which are three times lower than the mobility found in the literature.[5,9,11] The values of $\beta_1 - \delta \sim 0.59$ and $\beta_2 - \delta \sim 0.57$ could suggest the presence of transport via topological surface states. However, as said before, the Rashba splitting of the Fermi surface of Bi_2Te_3 could also lead to a non-zero Berry phase. This will be discussed later in the text.

Angular dependence measurements are usually performed to indicate the 2D nature of the oscillation and to infer the possible contribution of TSS. If the SdH oscillations originate from 2D Fermi surface states, the maximum and minimum oscillations must be aligned with each other for different angles when the curves are plotted as a function of the perpendicular component of the magnetic field ($B_\perp = B\cos\theta$). Figure 4(a) shows the SdH oscillations at 4.2 K for different angular orientations plotted as a function of $1/B\cos\theta$. The sample holder is rotated with tilt angles θ, while the applied magnetic field is kept fixed in the z-direction (see the inset). At $\theta = 0$, we choose two maxima indicated by the dashed vertical lines to check how the

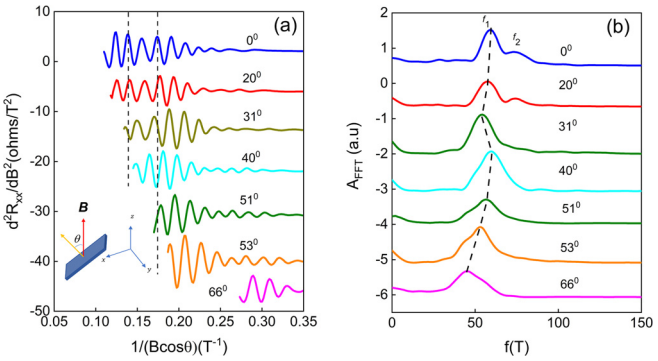

FIG. 4. (a) SdH oscillations at T = 4.2 K for different tilt angles θ plotted as a function of $1/B\cos\theta$. The inset shows the measurement configuration. (b) FFT curves of the respective oscillations in (a). The dashed line indicates the angular evolution of the SdH frequency f_1.

position of the peaks behaves as the angle changes. As θ varies from 0° to 66°, the maximum positions change from the original positions. This behavior indicates that the observed SdH oscillations cannot be originated from 2D Fermi surface states. In addition, in the case of TSS, the frequencies obtained from FFT must follow the dependence $f \propto 1/\cos\theta$, and f_1 must increase as θ increases, which is clearly not the case, as indicated by the dashed line in Fig. 4(b). This behavior also indicates that the shape of the Fermi surface is not spherical nor cylindrical and is in a transition from a closed ellipsoid to an open Fermi surface.[6] The behavior of f_2 cannot be verified since it disappears for tilt angles higher than 20°. The angular dependence deviation of f_1 from the 2D behavior indicates that the SdH oscillation with frequency f_1 originates from 3D bulk states. In fact, similar behavior was observed in Bi_2Se_3[12] and BiTeCl,[13] which have the same layered structure. In the case of BiTeCl, the anomalous behavior of $f(\theta)$ is due to its Fermi surface shape that varies from spindle torus to ring torus, depending on the carrier concentration. For Bi_2Se_3, the Fermi surface can change from pure ellipsoidal to the bag shaped surface, also depending on carrier concentration. The Fermi surface of Bi_2Te_3 has been investigated and revealed a very complex structure,[14] which can even diverge from the surfaces allowed to Bi_2Se_3 and BiTeCl and lead to anomalous behavior of $f(\theta)$.

As previously indicated in the text, the Rashba effect can also be responsible for the two peaks observed in the FFT transform [Fig. 3(a)] and can lead to a non-zero Berry phase. The appearance of two frequencies with the same profiles as those observed in Fig. 3(a) has been observed in several systems, including bulk BiTeCl,[13] SnTe epilayer,[15] $InSb/In_{1-x}Al_xSb$,[16] and HgTe quantum wells,[17] and attributed to the Rashba spin-splitting. For Bi_2Te_3 single crystals, a similar profile has also been observed recently, but its origin has not been addressed.[5] We consider that, for the analysis presented next, the Rashba spin splitting is responsible for the frequency f_2 obtained from the SdH oscillations.

In the absence of Rashba splitting, the cross-sectional area of the Fermi surface S_F perpendicular to the applied magnetic field gives rise to a cyclotronic frequency according to Onsager relation $f = (\hbar/2\pi e)S_F$ [see Fig. S2(a), in the supplementary material]. If the Rashba effect is present, the spin-splitting of Fermi surface produces two apparent cross-sectional areas, an internal S_1 and an external S_2,

as illustrated in Fig. S2(b) of the supplementary material. These two Fermi pockets S_1 and S_2 can be related to the frequencies f_1 and f_2. A general circular cross-sectional area is given by $S_F = \pi k_F^2$. Using the frequencies f_1 and f_2, we derive the Fermi wave vectors and obtain $k_{F1} = 0.0423$ Å^{-1} e $k_{F2} = 0.0477$ Å^{-1}. The Fermi velocities obtained from these values are $v_{F1} = 1.07 \times 10^6$ m/s and $v_{F2} = 1.73 \times 10^6$ m/s, which are one order higher than the values found in the literature for bulk Bi_2Te_3 films.[1,5,9] The Rashba splitting in momentum space, Δk_R, can be calculated from geometric considerations taking into account the distance between the center of the two circles indicated in Fig. S2(b) of the supplementary material, leading to the value of $\Delta k_R \sim 0.009$ Å^{-1}. The Rashba energy can be calculated from $E_R = \hbar^2 \Delta {k_R}^2 / 2m_c$, which gives $E_R = 6.8$ meV. From these values, we can calculate the Rashba parameter $\alpha_R = 2E_R/\Delta k_R$, which gives $\alpha_R = 1.58$ eV Å. Similar investigations were performed on bismuth tellurium chloride (BiTeCl) and potassium doped Bi_2Se_3 single crystals. For BiTeCl, the Rashba parameters were $\Delta k_R \sim 0.030$ Å^{-1} and $\alpha_R = 1.2$ eV Å,[13] while for Bi_2Se_3:K, $\Delta k_R \sim 0.066-0.08$ Å^{-1} with $\alpha_R = 0.79 - 0.35$ eV Å.[18]

The observed Rashba splitting may be related to the intrinsic disorder present in the Bi_2Te_3 film or due to surface oxidation of the sample. It is well known that Bi_2Te_3 undergoes surface oxidation when exposed to an ambient environment due to the weak interlayer interaction.[11] Bando *et al.*[19] investigated the Bi_2Te_3 surface oxidation in controlled air conditions (30% relative humidity and 24 °C) and reported that an oxidized layer with a thickness of one quintuple layer (1 nm) is formed on the Bi_2Te_3 surface just after 50 h of air exposure. Therefore, as the Bi_2Te_3 film investigated here was exposed to air for a period of years before performing the magnetotransport measurements, we can assure that its surface is oxidized. A theoretical investigation showed that the adsorbed atoms from the atmosphere, such as Na and O, alter the surface states by inducing the Rashba splitting due to the charge transfer from the adsorbed atoms to the sample surface.[20] The Rashba parameters found in this work are summarized in Table I and compared to the data available in the literature.

We can also extract the Landé g factor from the oscillations if the magnetic field is sufficiently high to show the Landau level separation (see Fig. S3 in the supplementary material). Using the cyclotron mass values obtained from the FFT analysis, we obtained $g = 21$ and $g = 33$, for $m_c = 0.046\, m_e$ and $m_c = 0.032\, m_e$, respectively. These values are close to the values found in the literature (see Table I).

In summary, we presented the magnetotransport measurements performed on a 156 nm-thick Bi_2Te_3 epitaxial film. From the analysis of the data, we suggest that SdH oscillations originate from the bulk states rather than surface states since the angular dependence of the FFT amplitudes does not follow the expected 2D Fermi surface state behavior. In addition, the non-zero Berry phase is attributed to the Rashba splitting that breaks the spin degeneracy, giving rise to the two frequencies observed in the FFT graphics. We also found that the Rashba parameter α_R is very high when compared to similar structures as BiTeCl and potassium doped Bi_2Se_3. This opens the possibility of the application of a tunable Rashba effect, via environmental exposure, to the development of spintronic devices based on Bi_2Te_3.

TABLE I. The cyclotronic masses, Landè g-factors, and Rashba parameters found in this work compared to the data available in the literature.

	This work	References
m_{c2} (units of m_e)	0.032	0.058; 0.075[21]
m_{c1} (units of m_e)	0.046	0.08;[5] 0.09[22]
g	$g_1 = 33.3; g_2 = 23$	17,[22] 10–25[3]
Δk_R (Å)$^{-1}$	0.009	0.030[13] $(0.066 - 0.08)$[18]
α_R (eV Å)	1.58	1.2[13] $(0.35 - 0.79)$[18]

See the supplementary material for the detailed procedure used to obtain the Berry phases, the Landé g-factor, and the schematic representation of the Rashba splitting of the Fermi surfaces.

We would like to thank CAPES and CNPq (No. 307933/2013) for their financial support.

DATA AVAILABILITY

The data that support the findings of this study are available from the corresponding author upon reasonable request.

REFERENCES

[1] D.-X. Qu, Y. S. Hor, J. Xiong, R. J. Cava, and N. P. Ong, "Quantum oscillations and Hall anomaly of surface states in the topological insulator Bi_2Te_3," Science **329**(5993), 821–824 (2010).
[2] S. Charpentier, L. Galletti, G. Kunakova, R. Arpaia, Y. Song, R. Baghdadi, S. M. Wang, A. Kalaboukhov, E. Olsson, F. Tafuri *et al.*, "Induced unconventional superconductivity on the surface states of Bi_2Te_3 topological insulator," Nat. Commun. **8**(1), 2019 (2017).
[3] R. Dey, T. Pramanik, A. Roy, A. Rai, S. Guchhait, S. Sonde, H. C. P. Movva, L. Colombo, L. F. Register, and S. K. Banerjee, "Strong spin-orbit coupling and Zeeman spin splitting in angle dependent magnetoresistance of Bi_2Te_3," Appl. Phys. Lett. **104**(22), 223111 (2014).
[4] O. Concepción, V. M. Pereira, A. Choa, S. G. Altendorf, A. Escobosa, and O. de Melo, "The growth of Bi_2Te_3 topological insulator films: Physical vapor transport vs molecular beam epitaxy," Mater. Sci. Semicond. Process. **101**, 61–66 (2019).
[5] K. Shrestha, V. Marinova, B. Lorenz, and C. W. Chu, "Evidence of a 2D Fermi surface due to surface states in a p-type metallic Bi_2Te_3," J. Phys. **30**(18), 185601 (2018).
[6] E. Lahoud, E. Maniv, M. S. Petrushevsky, M. Naamneh, A. Ribak, S. Wiedmann, L. Petaccia, K. B. Chashka, Y. Dagan, and A. Kanigel, "Evolution of the Fermi surface of a doped topological insulator with carrier concentration," Phys. Rev. B **88**(19), 195107 (2013).
[7] F. Nichele, M. Kjaergaad, H. J. Suominen, R. Skolasinski, M. Wimmer, B.-M. Nguyen, A. A. Kiselev, W. Yei, M. Sokolich, M. J. Manfra *et al.*, "Giant spin-orbit splitting in inverted InAs/GaSb double quantum wells," Phys. Rev. Lett. **118**(1), 016801 (2017).
[8] C. I. Fornari, P. H. O. Rappl, S. L. Morelhão, and E. Abramof, "Structural properties of Bi_2Te_3 topological insulator thin films grown by molecular beam epitaxy on (111) BaF_2 substrates," J. Appl. Phys. **119**(16), 165303 (2016).
[9] S. Barua, K. P. Rajeev, and A. K. Gupta, "Evidence for topological surface states in metallic single crystals of Bi_2Te_3," J. Phys. **27**(1), 015601 (2015).
[10] J. Xiong, Y. Luo, Y. Khoo, S. Jia, R. J. Cava, and N. P. Ong, "High-field Shubnikov–de Haas oscillations in the topological insulator Bi_2Te_2Se," Phys. Rev. B **86**(4), 045314 (2012).
[11] P. Ngabonziza, Y. Wang, and A. Brinkman, "Bulk contribution to magnetotransport properties of low-defect-density Bi_2Te_3 topological insulator thin films," Phys. Rev. Mater. **2**(4), 044204 (2018).
[12] L. Fang, Y. Jia, D. J. Miller, M. L. Latimer, Z. L. Xiao, U. Welp, G. W. Crabtree, and W.-K. Kwok, "Catalyst-free growth of millimeter-long topological insulator Bi_2Se_3 nanoribbons and the observation of the π-Berry phase," Nano Lett. **12**(12), 6164–6169 (2012).

[13]F. X. Xiang, X. L. Wang, M. Veldhorst, S. X. Dou, and M. S. Fuhrer, "Observation of topological transition of Fermi surface from a spindle torus to a torus in bulk Rashba spin-split BiTeCl," Phys. Rev. B **92**(3), 035123 (2015).
[14]S. J. Youn and A. J. Freeman, "First-principles electronic structure and its relation to thermoelectric properties of Bi_2Te_3," Phys. Rev. B **63**(8), 085112 (2001).
[15]A. K. Okazaki, S. Wiedmann, S. Pezzini, M. L. Peres, P. H. O. Rappl, and E. Abramof, "Shubnikov–de Haas oscillations in topological crystalline insulator SnTe(111) epitaxial films," Phys. Rev. B **98**(19), 195136 (2018).
[16]A. M. Gilbertson, W. R. Branford, M. Fearn, L. Buckle, P. D. Buckle, T. Ashley, and F. Cohen, "Zero-field spin splitting and spin-dependent broadening in high-mobility $InSb/In_{1-x}Al_xSb$ asymmetric quantum well heterostructures," Phys. Rev. B **79**(23), 235333 (2009).
[17]C. R. Becker, X. C. Zhang, A. P. Jeschke, K. Ortner, V. Hock, G. Landwehr, and L. W. Molenkamp, "Very large Rashba spin-orbit splitting in HgTe quantum wells," J. Supercond. **16**(4), 625–634 (2003).
[18]Z.-H. Zhu, G. Levy, B. Ludbrook, C. N. Veenstra, J. A. Rosen, R. Comin, D. Wong, P. Dosanjh, A. Ubaldini, P. Syers *et al.*, "Rashba spin-splitting control at the surface of the topological insulator Bi_2Se_3," Phys. Rev. Lett. **107**(18), 186405 (2011).
[19]H. Bando, K. Koizumi, Y. Oikawa, K. Daikohara, V. A. Kulbachinskii, and H. Ozaki, "The time-dependent process of oxidation of the surface of Bi_2Te_3 studied by x-ray photoelectron spectroscopy," J. Phys. **12**(26), 5607–5616 (2000).
[20]K. H. Jin and S. H. Jhi, "Effect of atomic impurities on the helical surface states of the topological insulator Bi_2Te_3," J. Phys. **24**(17), 175001 (2012).
[21]A. Wolos, S. Szyszko, A. Drabinska, M. Kaminska, S. G. Strzelecka, A. Hruban, A. Materna, and M. Piersa, "Landau-level spectroscopy of relativistic fermions with low fermi velocity in the Bi_2Te_3 three-dimensional topological insulator," Phys. Rev. Lett. **109**(24), 247604 (2012).
[22]C. W. Rischau, B. Leridon, B. Fauqué, V. Metayer, and C. J. van der Beek, "Doping of Bi_2Te_3 using electron irradiation," Phys. Rev. B **88**(20), 205207 (2013).